

RESEARCH ARTICLE

The flexural and shear behavior of SIFCON concrete beams with steel and GFRP bars

Barış Bayrak^{1*}

¹ Kafkas University, Department of Civil Engineering, Kars, Türkiye

Article History

Received 15 August 2023 Accepted 13 September 2023

Keywords

SIFCON

Glass-fiber reinforced fiber (GFRP) Steel fiber Shear behavior Flexural behavior, RC beam

Abstract

The SIFCON concrete reinforced with glass-fiber reinforced polymer (GFRP) bars can provide a construction system with high durability and strength. Slurry infiltrated fibrous concrete (SIFCON) is a new type of conventional fiber reinforced concrete. The aim of this paper is to evaluate the flexural and shear behavior of the SIFCON concrete beams reinforced with GFRP bars were evaluated under fourpoint bending and three-point shear tests. The parameters investigated were material type of longitudinal reinforcement (steel and GFRP), transverse reinforcement type (steel and mesh) and mesh reinforcement spacing (25 mm and 12 mm). For this purpose, a total of twelve SIFCON concrete beams with steel and GFRP bar as longitudinal reinforcement measuring 150x150x800 mm were cast. Moreover, stirrup and mesh reinforcement as transverse reinforcement are another main parameter of this study. The test results showed that the effects of longitudinal and transverse reinforcement type and mesh spacing on the strength, crack propagation, and energy dissipation capacity of RC beams under bending and shear were experimentally investigated. The use of steel longitudinal reinforcement in both four-point and three-point tests increased the bending moment and shear strength compared to beams with GFRP. Moreover, although the use of mesh reinforcement in reinforced concrete beams under four-point bending reduced the strength, it increased the strength in beams with GFRP. In the samples under the shear force, the use of mesh reinforcement in the steel reinforced group increases the shear strength, but the use of mesh reinforcement in the GFRP group decreases the shear strength.

1. Introduction

Concrete is one of the most-used construction materials because of a lot of advantages such as high compressive strength, good durability and lower cost. However, in spite of these advantages, concrete also has disadvantages such as low tensile strength, brittleness, low deformation capacity and load bearing strength after cracking etc [1-3]. On the other hand, the weak properties of concrete can be improved with the help of different materials. Among these disadvantages of concrete, brittleness is the most important problem. Using fiber in mixture is a solution to eliminate the brittleness properties of concrete. The using of steel fibers improves the tensile strength, flexural strength, toughness, ductility, dissipation energy capacity

eISSN 2630-5763 © 2023 Authors. Publishing services by golden light publishing®.

^{*} Corresponding author (<u>bbayrak@kafkas.edu.tr</u>)

and fatigue resistance. The use of fiber between 1% and 3% is the most common fiber volume ratio in conventional fiber reinforced concrete [4-8]. Because, increasing the fiber ratio in the mixture decreases the workability of concrete. But although the fiber ration in mixture is typically between %1 and %3, the volume ratio of fiber ranging from %3 to %20 is used in several specific concrete types such as the slurry infiltrated fiber concrete (SIFCON).

SIFCON that was produced by Lankard [9] in 1984 at Materials Laboratory, Columbus, Ohio, USA and consists of cement based slurry or flowing mortar is the new high-performance concrete type that is manufactured with high fiber ratio and differs from conventional fiber reinforced concrete in terms of production and composition and exhibits good mechanical properties such as high compressive, tensile, flexural and shear strength as well as high toughness and dissipation energy capacity [4, 10]. SIFCON consists of flowing mortar, fine sand, water, chemical additives and high ratio of fiber. Compared to conventional concrete, the coarse aggregate is not use in SIFCON mixture [11-13]. Because the coarse aggregate cannot reach all small spaces of matrix and between the fibers. In addition, SIFCON can contain some mineral additives such as fly ash, silica fume and slag. There is no harm in using these materials in mixtures as they have small diameters and increase the compressive strength. On the other hand, although the fiber ratio that is widely used in SIFCON ranges between %3 and %20, some researchers can get up to %30 fiber ratio. Because of these properties, SIFCON is a modern type of fiber reinforced concrete.

The mechanical properties of SIFCON such as compressive, tensile and flexural strength are higher than those of conventional concrete and conventional fiber reinforced concrete. Furthermore, there are effects of the properties of used fiber such as the kind of fiber (steel, polypropylene, glass, etc.), fiber ratio, fiber shape, the aspect ratio of fiber, alignment, tensile and elastic modulus of fiber on the mechanical properties of SIFCON [4, 14-16]. Several types of fiber such as steel, glass polypropylene and a new type of fiber polyolefin can be used in SIFCON mixture. On the other hand, the defense structures, safe vaults, industrial floors, pavements, strengthening and retrofitting works, seismic resistant structures and military structures are some potential usage areas of SIFCON due to their high energy dissipation capacity, high impact resistance [1]. However, the use of SIFCON in these areas has been limited due to quality control and its high cost.

One of the most important problems with structures such as RC roads, bridges and foundations etc. exposed to aggressive environments is corrosion of reinforcement. The strength of steel reinforcement decreased after being exposed to corrosion. In addition, because of corrosion of steel reinforcement, the strength of RC members decreased and the cracking of RC members increased. One of the ways to avoid this problem is to use a material that is more resistant to corrosion instead of steel reinforcement. On the other hand, one of the disadvantages of steel is the carbon dioxide (CO₂) emission problem. 1.85 CO₂ for every ton of steel produced releases into the atmosphere the process of manufacturing steel. The third industry is the steel industry which has one of the largest carbon footprints. Hence, an eco-friendly type of reinforcement such as FRP is needed for use in the construction industry [17-20]. The use of FRP bars as an alternative to steel reinforcement is a new method that has been used recently. FRP bars are divided into several groups according to the type of fiber and the most commonly used FRP types in the literature are Aramid Fiber Reinforced Polymer (AFRP), Basalt Fiber Reinforced Polymer (BFRP), Carbon Fiber Reinforced Polymer (CFRP) and Glass Fiber Reinforced Polymer (GFRP). The FRP bars have different mechanical properties. Moreover, the other advantages of FRP bars are their high tensile strength and light weight. The low density of FRP bars also causes the weight of the structural member to be reduced. Thus, since the weight of the structure is reduced, the effect of earthquake forces on the structure is also reduced. In order to take advantage of FRP bars, the concrete compressive strength must also be high. Otherwise, the concrete reached failure mode before not being utilized to maximum capacity of FRP bars. And also, this is not an economical way to use between FRP and conventional concrete [17, 21, 22]. In order to take advantage

of FRP bars, it is better to use FRP bars together with ultra-high performance concrete and SIFCON than conventional concrete.

The advantages of GFRP are its high tensile strength, corrosion resistance and small dead weight. The other advantage of GFRP is that it is a more cost-effective solution than other types of FRP bars. Because of high strength, lightweight, electromagnetic transparency, fatigue resistance of GFRP bars, it has an increasing trend among researchers [23, 24]. On the other hand, GFRP bars have been used on a lot of buildings such as bridges, marine structures, offshore structures. GFRP bars have high modulus of elasticity, in the range of 35 GPa and 51 GPa. The modulus of elasticity of GFRP is higher than that of conventional steel reinforcement, approximately %20 [24].

In recent years of literature review about SIFCON and the beams with FRP/GFRP, different studies have been carried out on the mechanical, physical, durability properties of SIFCON and flexural/shear behavior of beams with FRP/GFRP. Jerry and Fawzi [25] investigated the impact resistance and density properties of SIFCON. The steel fiber and polyolefin fibers were added to the SIFCON mixture. Moreover, they claimed that the polyolefin fiber was used for the first time at SIFCON. The researchers indicated that the use of polyolefin fiber and steel fiber decreased the cost and increase the impact resistance of SIFCON. Sampath and Asha [26] carried out an experimental program about mechanical properties of SIFCON produced with different fiber ratios (5%, 15%, 25% and %35). They stated that the increase in the steel fiber ratio increased the compressive and tensile strength. Sengul [27] investigated the mechanical properties of SIFCON containing waste steel fibers obtained from scrap tires. The diameters of waste steel fibers are between 0.18 mm and 2 mm. Furthermore, the length of waste steel fibers is between 41 mm and 208 mm. The waste steel fiber ratios were selected as 0%, 0.5%, 1%, 2%, 3%, 4% and 5%. The researchers found that the maximum 5% fiber ratio was not enough for SIFCON mixture. However, they indicated that placing the higher amount of fiber into the mold was impossible because the bulking of waste fiber on the mold was a serious problem. As a result, the flexural and compressive strength increased with increasing waste steel fiber ratio. So the researchers highlighted that the waste steel fiber can be use in SIFCON mixture. Aygörmez et al. [28] studied the mechanical properties of SIFCON containing fly ash, metakaolin and 5% steel fiber. The test results indicated that adding metakaolin to mixture increased the mechanical properties of SIFCON. Al-Salim et al. [29] investigated the energy dissipation capacity of SIFCON in flat slab-column connection. Test results indicated that using SIFCON in flat slab-connection decreased the energy dissipation capacity. Dong et al. [30] investigated the behavior of circular GFRP reinforced alkali-activated fly ash/slag column and beams under combined loading. GFRP spiral bars as transverse reinforcement were used in column and beam samples. The test parameters are the number of longitudinal reinforcements, the spiral pitch, the material of longitudinal reinforcement and load eccentricities. They found that using GFRP bars decreased the load capacity while increasing the ductility compared to steel reinforcement. Ahmed et al. [31] carried out an experimental study about the fly ash based geopolymer concrete reinforced with GFRP and CFRP bars of beams under four-point bending. The test parameters are longitudinal reinforcement ratio and type (as GFRP and CFRP). The researchers found that the ultimate load capacity of beam with CFRP bars is higher than beam with GFRP bars, and the crack width of beam with GFRP bars is more extensive than beam with CFRP. Moreover, the deflection capacity for same corresponding load level of beam with GFRP is higher than beam with CFRP. Wang and Belardi [32] studied the flexural behavior of beams with FRP bars (GFRP and CFRP) and fiber reinforced concrete (polypropylene). As a result of test dates, the crack width of beam with FRP and fiber reinforced concrete is smaller than beam with FRP and conventional concrete. Maranan et al. [33]carried out an experimental study on the flexural behavior (four-point bending) of RC beams with geopolymer concrete reinforced with GFRP bars. The effect of nominal bar diameter, reinforcement ratio and anchorage system on the flexural behavior were evaluated by researchers. The test results showed that bar diameter has no effect on the flexural performance but increasing reinforcement ratio increased the

serviceability performance of tested samples under bending moment. Adam et al. [34] carried out an experimental, analytical and numerical investigation of the beam with GFRP bars under flexural behavior. In terms of analytical and numerical study, the non-linear finite element analysis was used to compare experimental and analytical test results and the proposed formulas for strength prediction of beam with FRP bars were used to compare experimental and numerical test results. The effects of reinforcement material type (GFRP and steel), concrete compressive strength and reinforcement ratio on the flexural behavior were studied by researchers. As a result, the strain of GFRP bars reached to 90% of the ultimate strains. On the other hand, the researchers examined that a good agreement between the experimental and numerical test results was reached. In addition, researchers proposed a formula to predict the effective moment of inertia of beams with GFRP bars, which is coherent with the formulas that are proposed in relevant codes. El-Nemr et al. [35] evaluated the effects of different parameters of GFRP bars on the behavior of beams under bending moment in a different way. The effect of modulus of elasticity (46.4 GPa and 69.3 GPa) and surface profile (sand-coated and helically-grooved) on GFRP bars was decided on main parameter of study. The test results showed that the sand-coating of GFRP is more effective at reducing cracking behavior than helically-grooved profiles.

There are a lot of studies in the literature about the flexural and shear performance of GFRP-RC beams. Whereas, few studies have investigated the performance of SIFCON concrete beams with GFRP bars. The objective of this study is to evaluate the performance of SIFCON concrete RC beam reinforced with steel and GFRP bars. Twelve beams (six beams under bending moment and six beams under shear force) measuring 150 mm wide×150 mm deep×800 mm long were cast with SIFCON concrete with steel fiber. The four-point bending and shear tests were conducted to assess flexural and shear behavior such as crack initiation, crack propagation, failure mode, load-deflection relationship and energy dissipation capacity. Moreover, two different types of mesh reinforcement, 25 mm and 12 mm mesh spacing, were used as horizontal reinforcement. The outcomes of this work can be used by engineers/designers to design the SIFCON concrete with steel fiber RC beams with steel and GFRP bars.

2. Experimental program

Experimental work contains two main group of beams with 150 mm depth, 150 mm width and 800 mm length. The first group (F) contains six beams that were subjected to flexural moment, while second group (S) contains six beams that were subjected to shear force. The SIFCON was used to all specimens. F-S, F-G, F-M and F-2M were reinforced with both steel and GFRP bars (steel (S) fiber) and different type of horizontal reinforcement (conventional stirrup, mesh reinforcement). Also, two types of dimension with 12 mm×12 mm×0.9 mm (M) and 25 mm×25 mm×1.8 mm (2M) were used as transverse reinforcement. The tested specimens were demolded after 24 hours of casting and marked. All specimens were cured in laboratory ambient and room temperature for 28 days.

2.1. Materials

2.1.1. SIFCON

SIFCON mix used in this study was composed of fine sand, design water, plasticizer, cement, steel fiber. Ordinary Portland cement CEM I-42,5R manufactured in Erzurum/Turkey, which was in conformity with TS EN 197-1 [36] standard was used in SIFCON mixture. The specific gravity and blaine specific surface of cement were 3.11 gr/cm³ and 3600-3900 cm²/gr, respectively. The mechanical and physical properties of cement are provided in Table 1. The range of 0-2 mm diameter sand was used as fine aggregate. The commercial product (Master Glenium ACE 450) superplasticizer was used in this study. The properties of superplasticizer are shown in Table 2. The tap water is used for mixing and curing. Hooked end steel of 30

mm length was used in the SIFCON mixture. Steel fiber was used in the mixture at a rate of 7% by volume. The mechanical and physical properties of steel fiber were shown in Table 3. The morphology of the steel used in the mixture is shown in Fig. 1. The mixture composition for 1 m³ is presented in Table 4.

Table 1. Mechanical and physical properties of cement

Mechanical properties (%)		Physical properties			
SiO ₂	19-20	Specific gravity (gr/cm ³)	3.11		
Al_2O_3	4-5	Blaine specific surface (cm ² /gr)	3600-3900		
Fe ₂ O ₃	3-3.5	Initial setting time (min)	150-180		
CaO	62-64	Final setting time (min)	190-220		
MgO	1-2	Compressive strength (MPa)	51-53		
SO ₃	3.20-3.80				
Na ₂ O	0.2-0.4				
K ₂ O	0.5-0.7				
Cl-	0.02-0.05				

Table 2. The properties of superplasticizer

Properties	
Material structure	Policarbocsilic ether
Appearance	Brown and fluid
Specific gravity (kg/lt)	1.069-1.109
pН	5-7
Alkali content (%)	<3.0
Chlorine content (%)	<0.1
Corrosion behavior	It contains only components that comply with the TS EN 934-1:2008 standard.

Table 3. Mechanical and physical properties of hooked end steel fiber

Fiber	Length (L) (mm)	Diameter (D) (mm)	Aspect ratio (L/D)	Density (kg/m3)	Tensile strength (MPa)
Steel	30	0.55	55	7850	1500

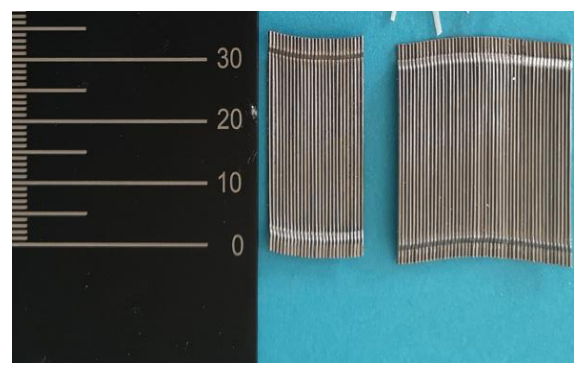


Fig. 1. Morphology of steel fiber

Table 4. Mixture composition of SIFCON for 1 m ³	Table 4.	Mixture com	position of	SIFCON f	or 1 m^3
---	----------	-------------	-------------	----------	--------------------

Materials	Mix proportion
Cement (kg/m³)	800
Fine aggregate (kg/m³)	935
Water (kg/m ³)	360
Superplasticizer (lt/m³)	16
Steel fiber (kg/m³)	550

2.1.2. GFRP bars and steel reinforcement

GFRP bars were made of alkali-resistant glass fiber (volume fraction >65%) and vinyl epoxy. The diameter and length of GFRP bars used as vertical reinforcement are 8 mm and 750 mm, respectively. The tensile and compressive strength of GFRP bar are 1200 MPa and 550 MPa, respectively. In addition, the density of GFRP is 1.80 gr/cm³. The 8-mm diameter deformed steel bars were used as longitudinal and transverse reinforcement. The stress-strain curves and mechanical properties of deformed steel rebar were shown in Fig. 2 and Table 5, respectively.

2.2. Test specimens

Six GFRP-reinforced and six steel-reinforced concrete beams were fabricated and tested. The all beams had dimensions of 150 mm width, 150 mm depth and 800 mm length and the concrete cover was 20 mm. The cross-sectional geometry and reinforcement details of beams were shown in Fig. 3. Two 8 mm diameter steel/GFRP bars were used for compression-zone reinforcement, are two 8 mm diameter steel/GFRP bars were used for tensile-zone reinforcement. The six tested beams were provided with 8 mm diameter steel stirrups spaced at 150 mm on-centers. The six tested beams were provided with two types of transverse reinforcement: 12 mm×12 mm×0,9 mm and 25 mm×25 mm×1.8 mm. The Turkish Standard (TS500-2000) [37] and ACI Code (ACI318-19) [38] were used to calculate the longitudinal and transverse reinforcement ratios in which the vertical and horizontal reinforcement ratios are 0.0052 and 0.0076, respectively. The test parameters of this study were type of longitudinal reinforcement (steel and GFRP reinforced), type of transverse reinforcement (steel stirrup and mesh reinforcement), test type (four-point flexure and three-point shear tests). Table 6 summarizes the label and classification of the tested beams. The tested beams were labeled based on the type of test, longitudinal reinforcement, transverse reinforcement. For example, the specimen identified as F-Steel-S- means that this specimen was tested under flexural (F) and was manufactured with steel steel longitudinal reinforcement (steel), steel transverse reinforcement (S).

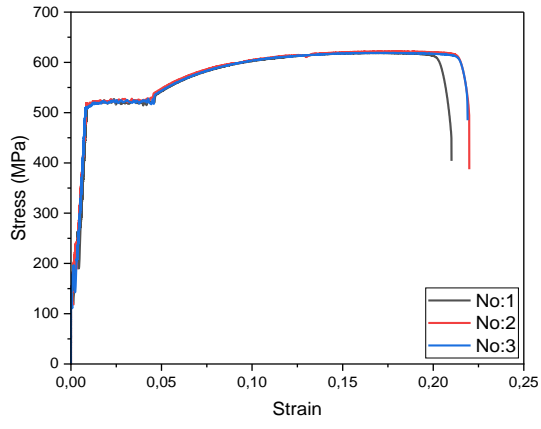


Fig. 2. Stress-strain curves of deformed steel bars

Table 5. Properties of deforme	ea stee	i bar
--------------------------------	---------	-------

	Tensile strength (MPa)	Tensile load (kN)	Yield strength (kN)	Length change (%)
No 1	630.18	31.67	532.05	21.65
No 2	626.63	31.49	520.38	20.02
No 3	622.31	31.28	521.38	20.82

Table 6. Properties of tested specimens

Groups	Specimen ID	Longitudinal reinforcing type	Transverse reinforcing type	
F* (flexural)	F/S*-Steel-S	Steel	Stirrup	
	F/S-GFRP-S	GFRP	Stirrup	
	F/S-Steel-S	Steel	Stirrup	
	F/S-GFRP-S	GFRP	Stirrup	
S* (shear)	F/S-Steel-12M	Steel	Mesh reinf. (12×12mm)	
	F/S-GFRP-12M	GFRP	Mesh reinf. (12×12mm)	
	F/S-Steel-25M	Steel	Mesh reinf. (25×25mm)	
	F/S-GFRP-25M	GFRP	Mesh reinf. (25×25 mm)	

^{*}If the bending moment acts on the specimen, the symbol "F" is used, if the shear force acts on the specimen, the symbol "S" is used.

2.3. Manufacture and casting of tested specimens

The testing of the specimens was carried out by utilizing a 60-liters mixer. Firstly, all dry materials such as cement and fine aggregate were mixed for 5 minutes. Then, 2/3 of the water and super plasticizer were added to the mixture and mixed for 3 minutes. Finally, 1/3 of the water was added and the mixture was mixed for another 3 minutes. After placing volume of 7% steel or glass fibers in the mold, the concrete mixture was poured into the molds (Fig. 4). At the time of concrete casting, three 100 mm×200 mm cylindrical specimens were taken for the compressive strength test, three 100 mm×200 mm cylindrical specimens for the splitting tensile test and three 70 mm×70 mm×280 mm prism specimens were taken for the flexural strength test. All samples were irrigated daily until the test day.

2.4. Hardened concrete test

Compressive strength and split tensile strength tests were performed on cylinders with 100 mm×200 mm in dimensions using a universal testing machine according to TS EN 12390-3 [39] and TS EN 12390-6 [40] the standards, respectively. Three cylindrical samples were examined at age of 28 days. The results of compressive strength and tensile strength are shown in Table 7. The flexural strength test was performed according to the TS EN 12390-5 [41] standard. The results of flexural test are shown in Table 8. Flexural strength curves of samples are shown in Fig. 5

2.5. Test setup and procedure

The four-point bending test and three-point test were employed to evaluate the flexural and shear performance of SIFCON concrete beams reinforced with steel and GFRP bars. The test setups and schematic diagrams are showed in Fig. 6. The experimental setup shown in Fig. 6a was used for the four-point bending test. The experimental setup shown in Fig. 6b was used for the shear test. The load was gradually applied over a simply supported beam with a shear span of 750 mm, through a spreader I-beam using a 1000 kN

capacity hydraulic jack at a rate of approximately 1 mm/min. A Linear Variable Differential Transformer (LVDT) was placed at midpoint to monitor the deflection.

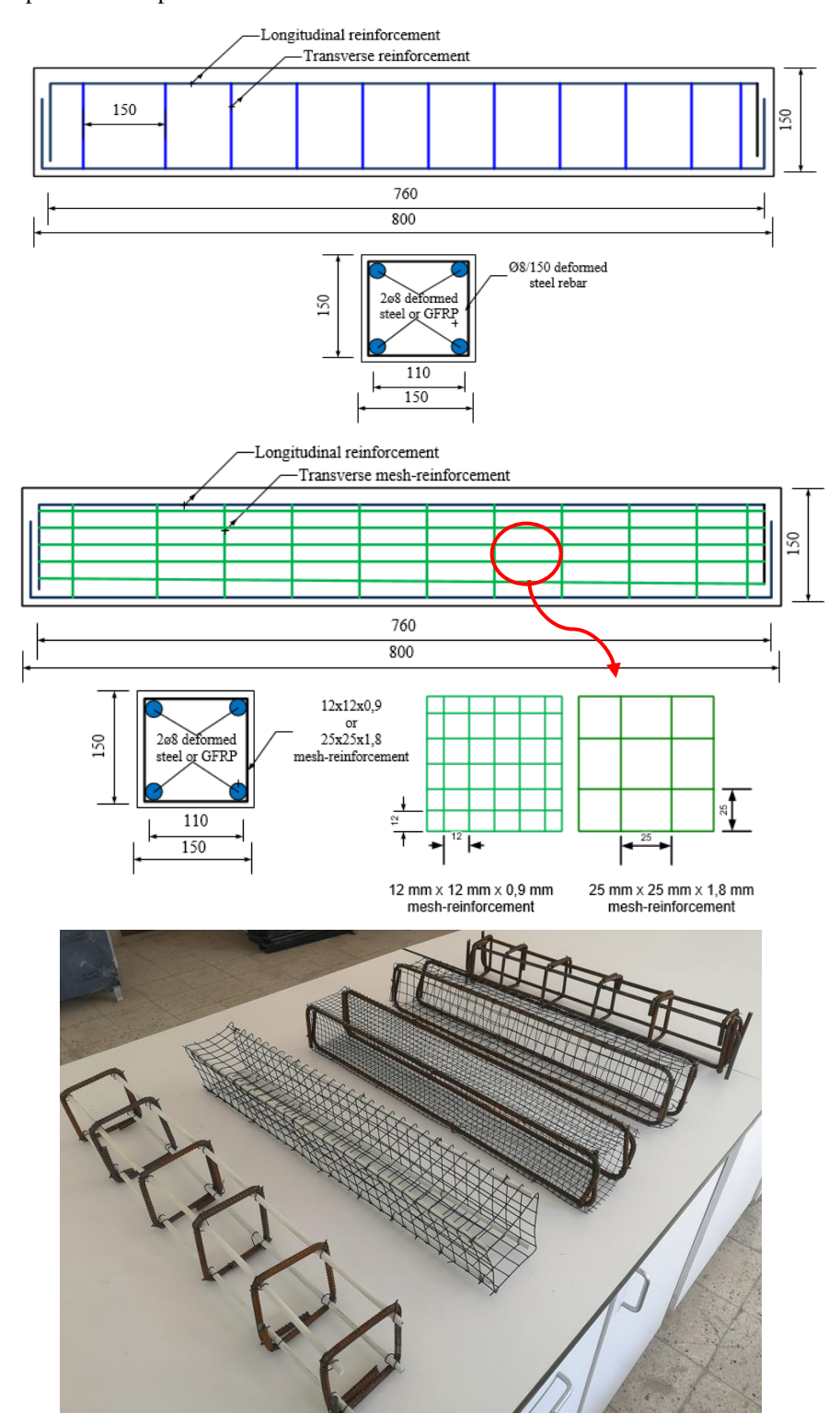


Fig. 3. Geometry and reinforcement details of beams (all units are mm)

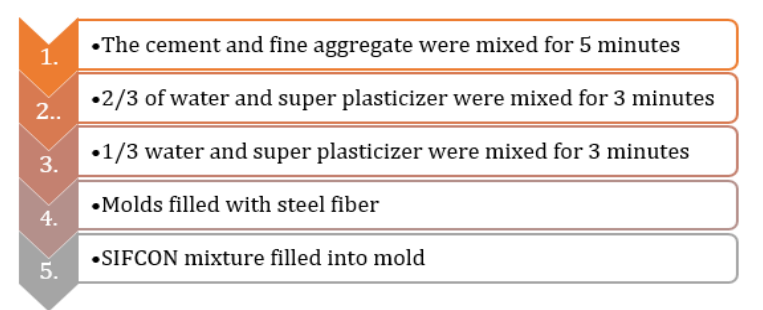


Fig. 4. Schematic representation of concrete pouring

Table 7. Results of the compressive strength, split tensile strength and flexural strength tests

Samples	Compressive strength (MPa) at 28 days	Split tensile strength (MPa) at 28 days	Flexural strength (MPa) at 28 days	
S1	51.25	4.87	16.09	
S2	52.67	5.12	19.31	
S3	53.32	4.97	21.52	
Avg.	52.41	4.98	18.97	

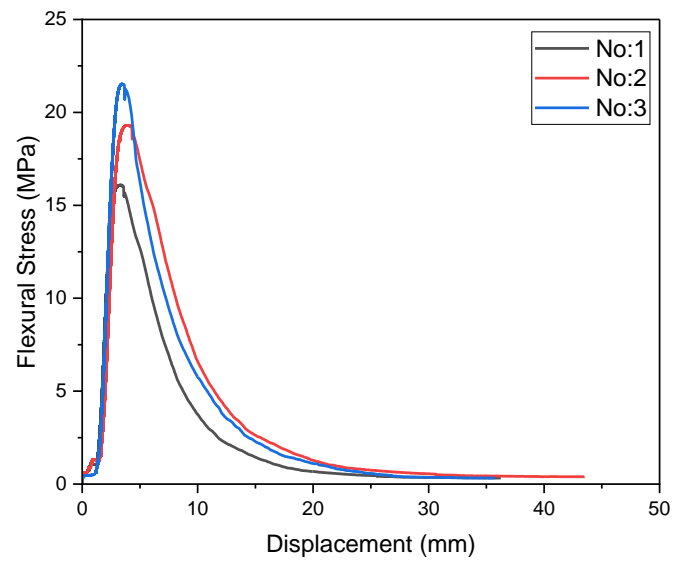


Fig. 5. Flexural strength of samples

3. Results

In this study, the effect of longitudinal and transverse reinforcement type on the bending and shear strength of RC beams produced from SIFCON was experimentally investigated. For this purpose, six RC beams were subjected to a four-point bending test to determine the bending strength and six RC beams were subjected to a three-point shear test to determine the shear strength.

3.1. Flexural behavior

The four-point bending test results are shown in Table 8. Table 8 shows the load at yield point (P_y) , maximum load (P_{max}) and ultimate load (P_u) and the corresponding displacement values at the relevant load. The load

at yield point is calculated as the point where the linearity of the load-displacement curve breaks down. The maximum load is taken as the pick point of the load-displacement curve. The ultimate strength is taken as the point at which there is a sharp load reduction in the specimens. Maximum and minimum load values were reached in F-Steel-S and F-GFRP-25MM samples, respectively. In the samples using steel as longitudinal reinforcement, the use of mesh stirrups instead of steel stirrups reduced the strength. However, in the samples using GFRP as longitudinal reinforcement, the use of mesh reinforcement increased the strength. The load capacity of the steel-reinforced specimens is higher than the GFRP-reinforced specimens, since the steel reinforcement provides better adhesion with the concrete. The additional advantages of steel fibers in samples using steel reinforcement can provide more deformation capacity under load. Generally, steel stirrups have a higher cross-sectional area in one piece, which can provide greater strength. Mesh reinforcements, on the other hand, consist of thinner wires and have a smaller cross-sectional area. Therefore, mesh reinforcements can provide lower strength under the same load compared to steel stirrups. Mesh reinforcements consist of finer wires and have a denser structure. This can make it difficult for them to be dispersed homogeneously into the concrete, thus affecting the load distribution. In the case that the mesh reinforcement is used with steel longitudinal reinforcements, the strength and load carrying capacity of the mesh reinforcement may be lower than the steel stirrups. Therefore, the use of mesh reinforcement with steel longitudinal reinforcement has reduced the flexural strength. GFRP bars can have high tensile strength and perform better than steel longitudinal reinforcement. When mesh reinforcement is used, the load bearing capacity of GFRP bars can be better evaluated, which increases the flexural strength.

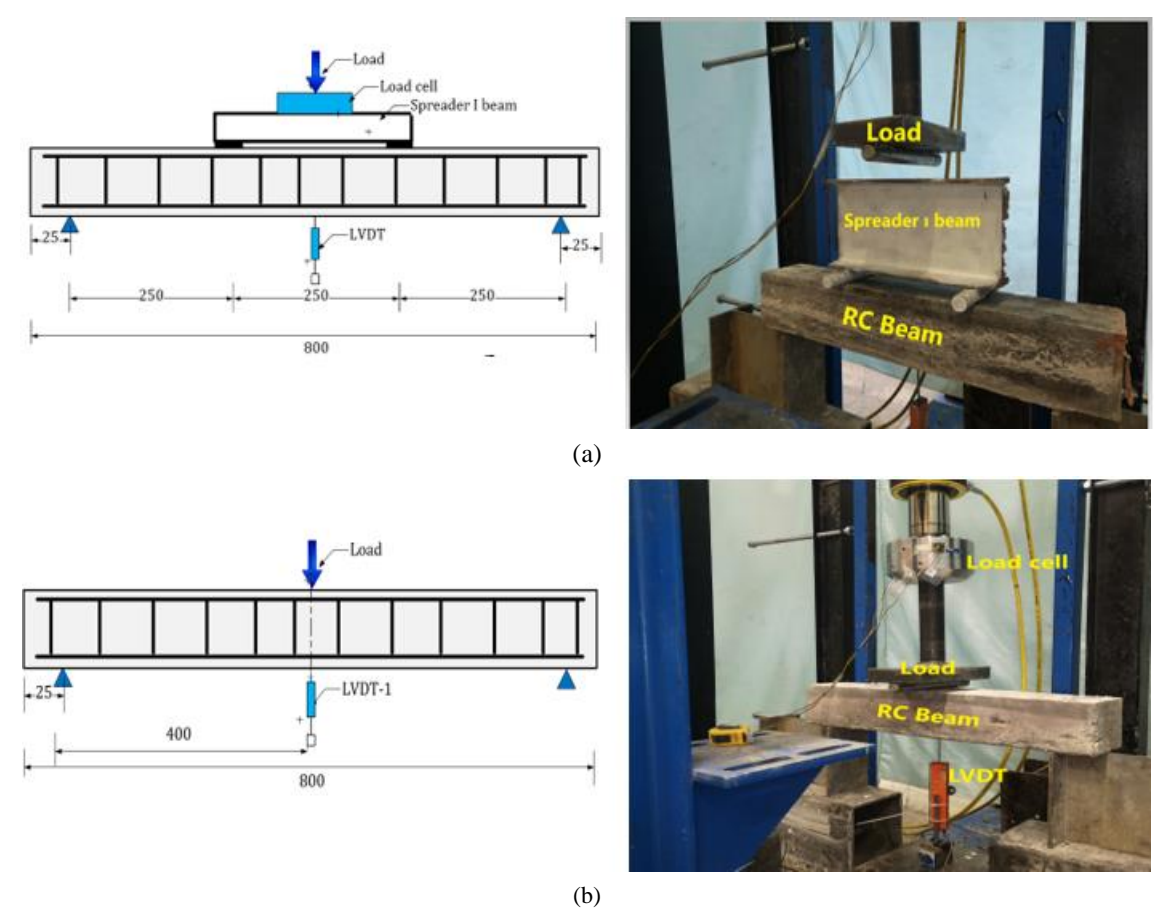


Fig. 6. Test setup a) four-point bending test setup b) three-point test setup

Moreover, the energy dissipation capacities of the samples are shown in Table 8. The energy dissipation capacity was calculated from the area under the load-displacement curve. F-Steel-S sample absorbed the most energy. F-Steel-S sample has 28.89% and 69.84% more energy absorption capacity than F-Steel-12M and F-Steel-25M samples, respectively. Since the ultimate displacement capacity of the F-GFRP-12M sample is low, its energy absorption capacity is also low compared to other samples.

Tabl	le 8	Flexural	test resul	lte
1 au	ic o.	TICXUIA	ICSL ICSU	11.5

Specimen	P _y (kN)	Δ _y (mm)	P _{max} (kN)	Δ _{max} (mm)	P _u (kN)	$\Delta_{\mathrm{u}} \left(mm \right)$	E (kN.mm)
F-Steel-S	117.60	6.06	125.44	8.64	90.74	23.17	2288.82
F-Steel-12M	101.86	6.90	104.04	7.79	21.05	28.42	1775.80
F-Steel-25M	90.00	7.87	99.16	9.85	66.00	19.47	1347.61
F-GFRP-S	26.43	5.43	47.39	7.71	38.66	20.62	853.25
F-GFRP-12M	65.85	3.94	66.49	5.71	28.61	10.55	490.41
F-GFRP-25M	84.39	14.67	87.31	17.14	41.68	26.92	1368.67

The load-displacement curves of the specimens are presented in Fig. 7. The load-displacement curves of the samples whose steel longitudinal reinforcement is shown in Fig. 7a and the load-displacement curves of the samples whose GFRP longitudinal reinforcement is shown in Figure 7b. Moreover, the comparison of load-displacement curves for all samples is shown in Fig. 8. In the samples using GFRP bar as longitudinal reinforcement, shark strength losses are seen after the maximum load is reached. Since there is no yield phenomenon in GFRP bars, there is usually no yield zone. Samples using GFRP bars showed a more brittle behavior. Since GFRP bars do not have a yielding zone, their deformation capacity is limited in samples where GFRP bars are used as longitudinal reinforcement.

The relationship between the unit weight and the load carrying capacity of the samples is shown in Figure 9. The use of mesh reinforcement and GFRP bars reduced the unit weight of the samples. In samples using steel longitudinal reinforcement, a direct proportional relationship is observed between load carrying capacity and unit weight. Whereas, in the samples where GFRP is used as longitudinal reinforcement, there is an inverse proportion between unit weight and load carrying capacity.

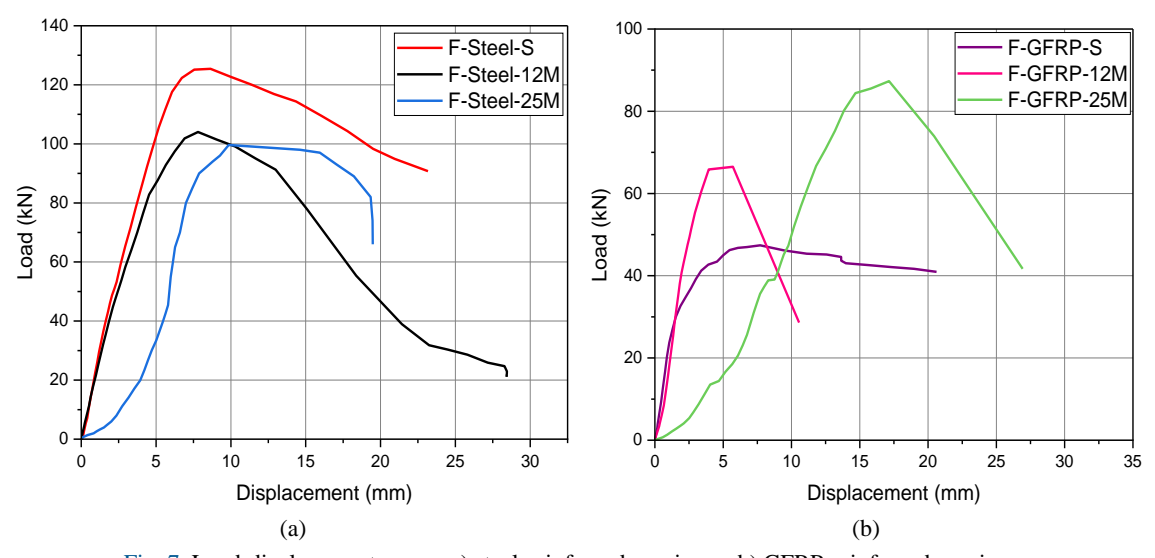


Fig. 7. Load-displacement curves a) steel-reinforced specimens b) GFRP-reinforced specimens

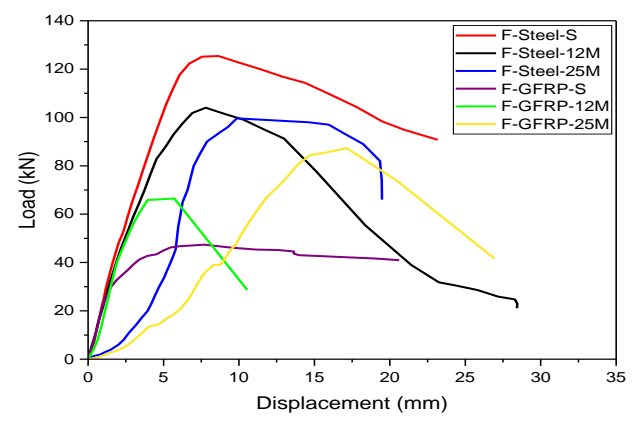


Fig. 8. Load-displacement relationship of all specimens under flexural moment

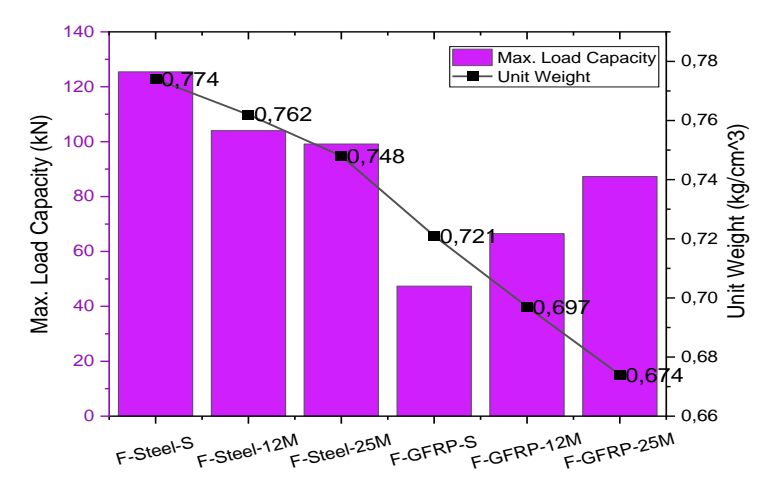


Fig. 9. Relationship between maximum load capacity under flexural moment and unit weight

Photographs of the specimens subjected to bending moment after the test are shown in Fig. 10. As can be seen from Fig. 10, the largest crack width was observed in the F-Steel-S sample. It was observed that the crack widths were higher in the samples in which steel was used as the longitudinal reinforcement. Structural damage is more, especially, in F-Steel-S and F-Steel-12M samples. These samples also have the highest load carrying capacity. Compared to the others, these samples also had more structural damage because they carried higher loads. It has been observed that the crack width that formed in the samples where GFRP bars are used as longitudinal reinforcement is wider compared to the samples with steel bars reinforced. Since less deformation occurred in the samples using GFRP, the crack width was observed to be less in these samples. In addition, more energy was dissipated by increasing the crack width in the samples using steel reinforcement. GFRP is a more brittle material than steel. This means that GFRP reinforced beams may tend to deform less under loading.

3.2. Shear behavior

The test results of specimens subjected to the shear force are shown in Table 9. The maximum shear strength was obtained in the S-Steel-12M sample. The use of mesh reinforcement led to an increase in shear strength in the samples where steel reinforcement was used. In the samples using GFRP reinforcement, the use of mesh reinforcement caused a decrease in shear strength. The shear strength of the samples using steel reinforcement is higher than the samples with GFRP reinforcement. It is thought that there is a lack of

adhesion between the concrete and the GFRP bars in the samples using GFRP. GFRP bars have a low modulus of elasticity, meaning they do not harden as much as steel reinforcement under shear force and exhibit more elastic deformation. When wire mesh is used as stirrups, the beam's ability to control horizontal cracks in the shear region may be limited. Since the elastic deformation of the mesh reinforcement is low, cracks spread more and reduce the shear strength. Therefore, the use of mesh reinforcement in GFRP reinforced beams reduced the shear strength. As can be seen from Table 9, the load at the yield point and the maximum load are very close to each other in the samples using GFRP bars. Since there is no yield phenomenon in GFRP bars, the two points are very close to each other. In Table 9, the energy dissipation capacities of the samples exposed to shear force are shown. The energy dissipation capacity of the samples using steel longitudinal reinforcement is higher than the samples using GFRP bars. Samples using steel reinforcement have higher energy dissipation capacities as they have both greater displacement capacity and load carrying capacity.

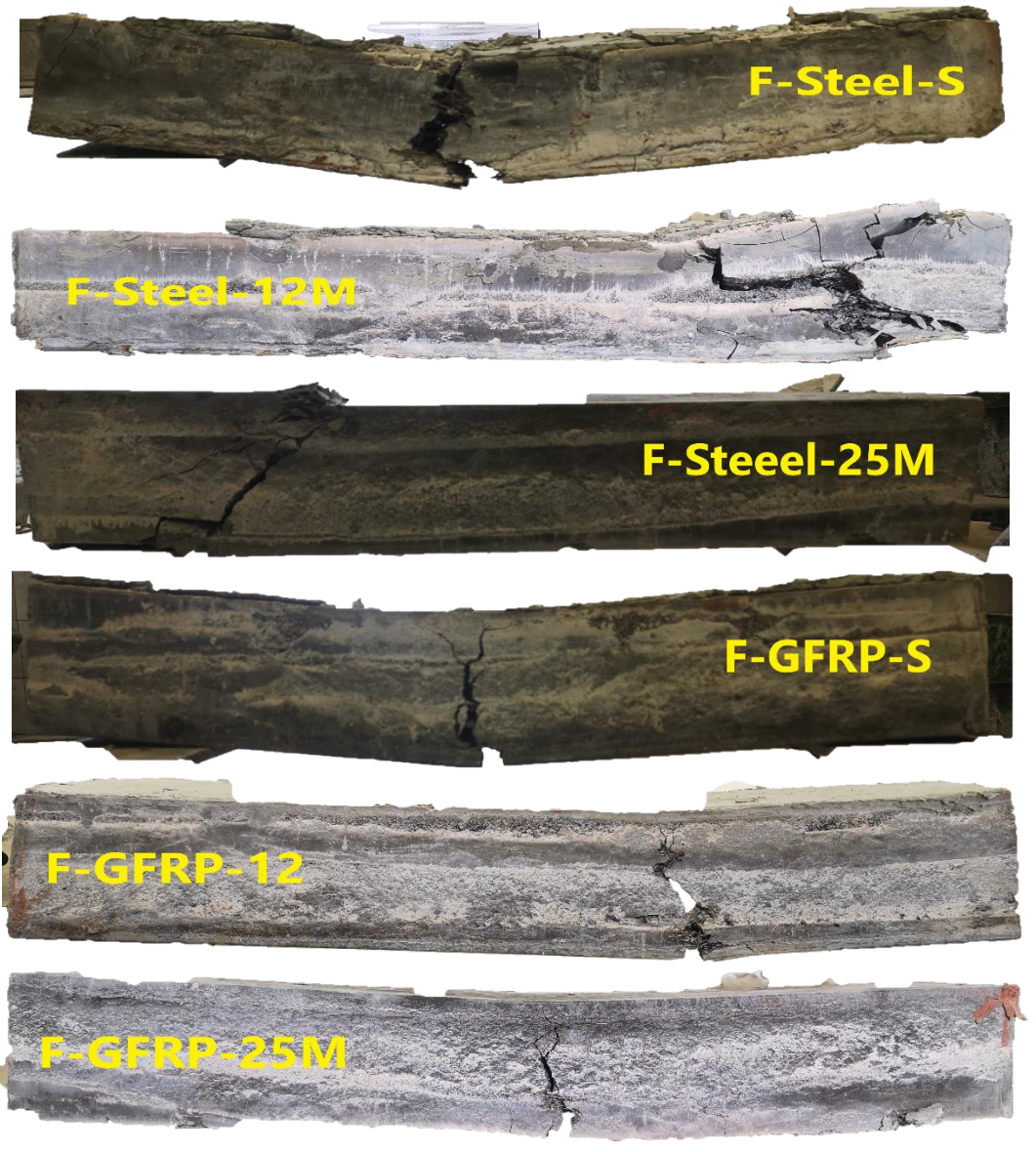


Fig. 10. Specimen photos after flexural test

Table 9. Shear tes	t results						
Specimen	$V_{y}\left(kN\right)$	Δ_y (mm)	$V_{max}\left(kN\right)$	Δ_{max} (mm)	$V_{u}\left(kN\right)$	$\Delta_u \ (mm)$	E (kN.mm)
S-Steel-S	74.57	6.74	75.22	7.67	51.78	25.00	1501.39
S-Steel-12M	81.98	5.03	86.39	5.62	52.15	32.19	2039.76
S-Steel-25M	82.40	6.09	84.84	6.93	57.06	35.41	2297.82
S-GFRP-S	47.44	5.57	48.12	6.58	23.02	27.15	895.09
S-GFRP-12M	40.92	3.24	41.84	3.76	12.14	35.12	746.95
S-GERP-25M	19 30	7.88	23.78	15 54	11.80	33.40	560.96

Table 9. Shear test results

The load-displacement graphs of steel and GFRP bar-reinforced specimens exposed to shear force are shown in Fig. 11a and b. The load-displacement curves of all specimens exposed to shear force are shown in Fig. 12. The displacement capacities of all samples are very close to each other. The forces within a beam are distributed differently as a result of increased loads. Parts of the beam may undergo increased stress and deformation as the load increases, while other regions may be relatively less affected. A closer fit between the displacement capabilities of steel and GFRP-reinforced beams than anticipated may result from this load redistribution's more balanced deformation behavior.

The relationship between the shear capacities and unit weights of the samples is shown in Fig. 13. Although there is an inverse proportionality between the unit weight and shear strength of the samples using steel reinforcement, there is a direct proportionality between the shear strength and unit weight of the samples using GFRP bar. In addition, the use of GFRP and mesh reinforcement has reduced the unit weight of the beams. As expected, the unit weight of the sample in which both the stirrup and the longitudinal reinforcement is steel has the highest value. In the samples using steel longitudinal reinforcement, using 12 mm and 25 mm spacing mesh reinforcement instead of steel stirrups reduced the unit weight by 1.52% and 3.88%, respectively. In beams using GFRP longitudinal reinforcement, the use of 12 mm and 25 mm mesh reinforcement instead of steel stirrups reduced the unit weight by 3.32% and 6.52%, respectively.

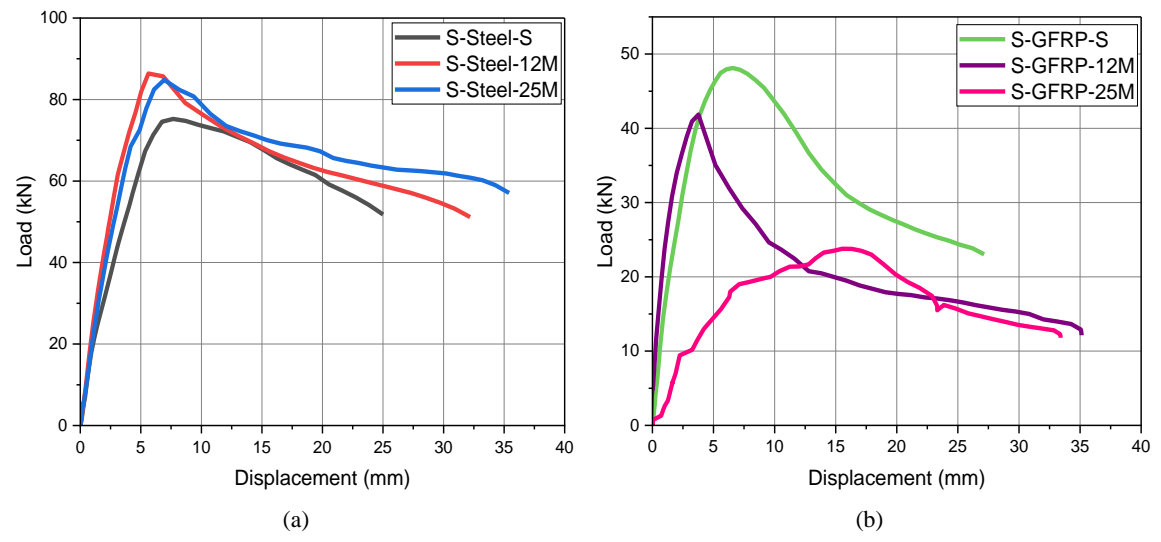


Fig. 12. Load-displacement curves a) steel-reinforced specimens b) GFRP-reinforced specimens

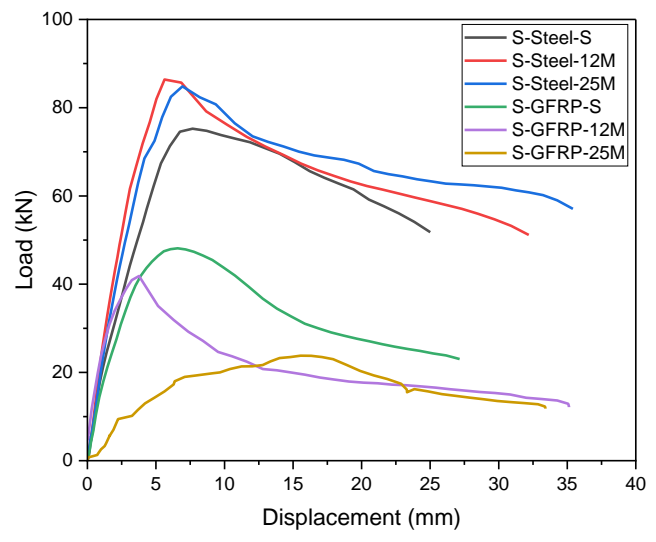


Fig. 12. Load-displacement relationship of all specimens under shear force

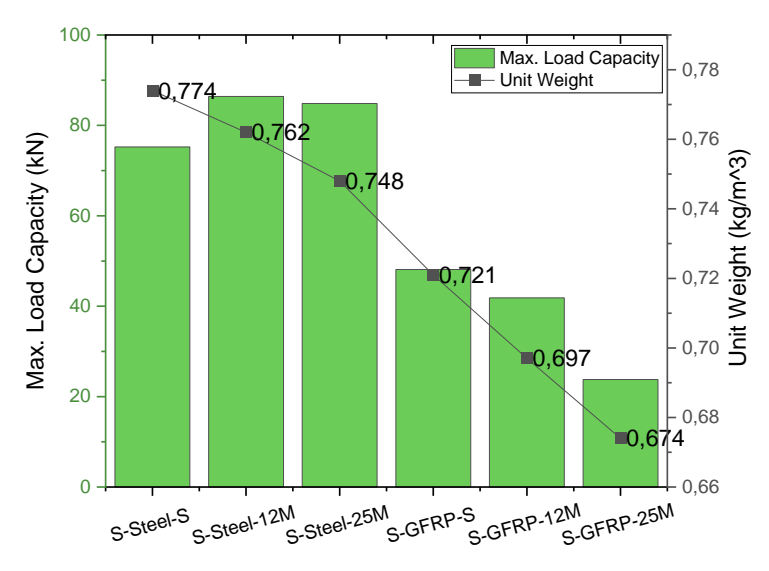


Fig. 13. force Relationship between maximum load capacity under flexural moment and unit weight

The pictures of the samples after the shear test are shown in Fig. 14. The maximum crack width was observed in the S-GFRP-S sample. It was observed that the crack distribution of the samples was close to each other. It was observed that the use of GFRP reinforcement and mesh reinforcement in the samples exposed to shear force did not have a significant effect on the crack distribution. After the first crack appeared in the test specimen, the crack width increased with the increasing load. The crack propagated upwards from the beam subregion. With the formation and propagation of the first crack, second and third cracks were observed in some beams.

3.3. Comparison of flexural and shear results

The results of flexural and shear test are shown in Fig. 15. The use of GFRP bars and mesh reinforcement in RC beams had a significant effect on both flexural and shear strengths. Except for two samples, the maximum load carrying capacity under shear force is greater than the load carrying capacity under bending moment in

other samples. The use of steel longitudinal reinforcement in samples under both bending moment and shear force increased the strength. The displacement values corresponding to the maximum load are close to each other under both bending moment and shear force. Differences were also observed between the ultimate displacement capacities of the samples under flexural moment and shear force and accordingly the energy dissipation capacities.

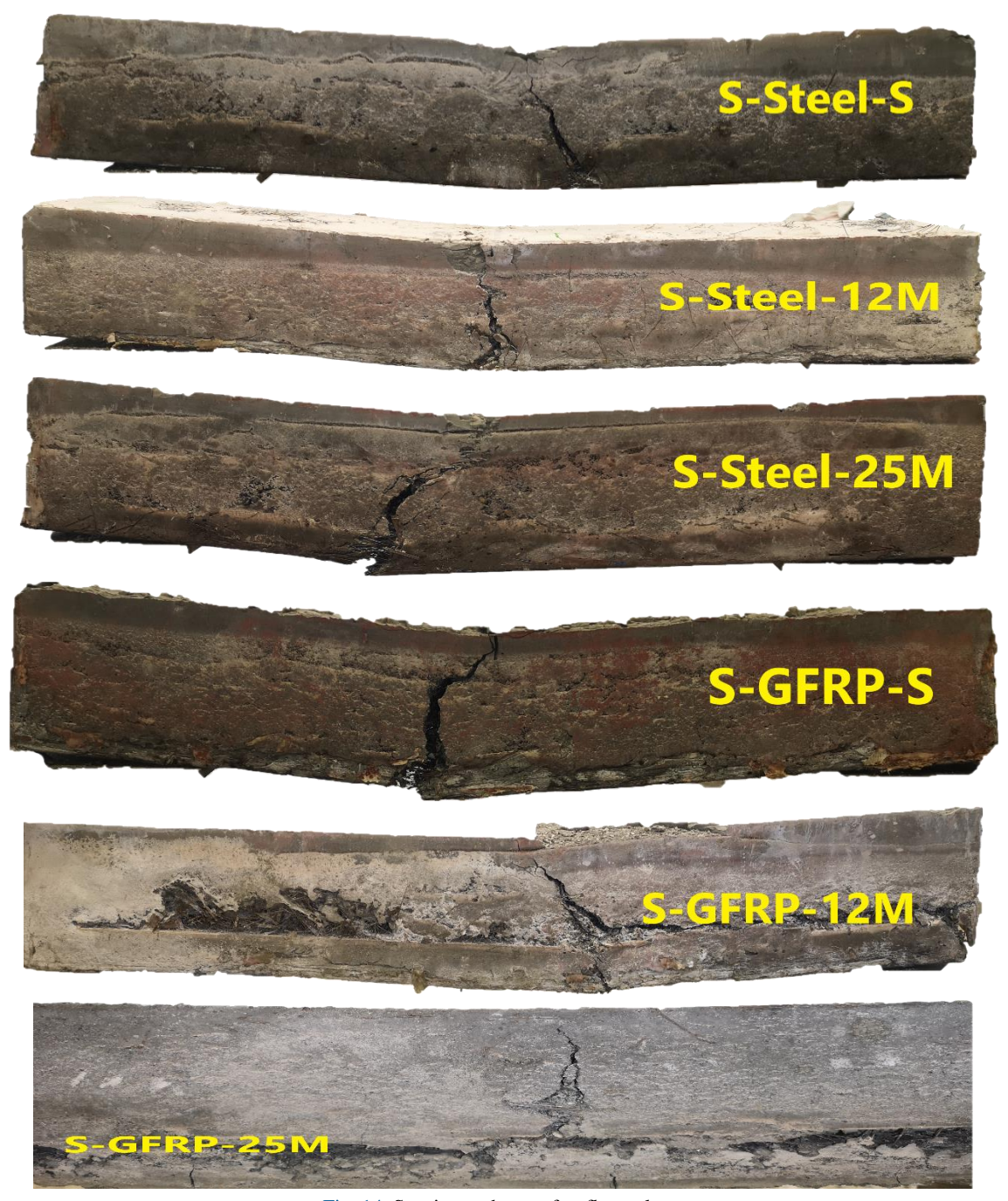


Fig. 14. Specimen photos after flexural test

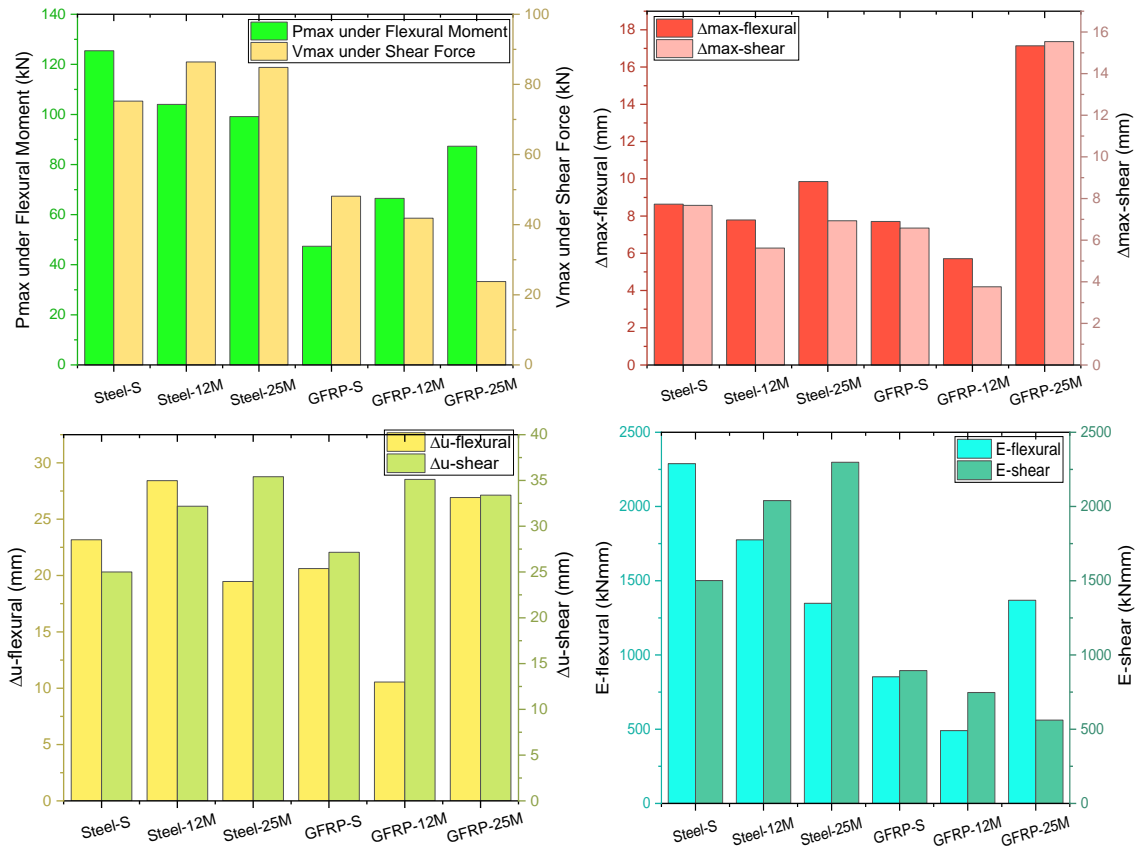


Fig. 15. Comparison of flexural and shear test results

In the samples using steel longitudinal reinforcement, the use of mesh reinforcement instead of steel stirrups caused the shear strength to be higher than the bending strength. The use of mesh reinforcement in GFRP reinforced beams caused the flexural strength to be higher than the shear strength. The effect of steel stirrups and mesh reinforcement in beams using steel longitudinal reinforcement was compared. Steel longitudinal reinforcement bears the main stresses of the beam, while mesh reinforcement often helps control crack formation near the surface of the beam.

It is associated with the ability of mesh reinforcement to control crack formation. Mesh reinforcement has increased the shear strength of the reinforced concrete element by preventing cracks. While steel stirrups are more effective in increasing bending strength because they carry the main stresses, mesh reinforcement can be more effective in controlling cracks and increasing shear strength. It can be attributed to the flexibility properties of GFRP and its ability to inhibit crack formation. The ability of mesh reinforcement to contain cracks, combined with the flexible structure of GFRP reinforcement, can increase flexural strength.

4. Conclusion

The aim of this study is to examine the effects of longitudinal and transverse reinforcement types on the flexural and shear strength of RC beams produced by using SIFCON concrete. 12 RC beams were subjected to flexure and shear tests. As a result of the study, the following findings were obtained.

 The use of both longitudinal and transverse reinforcement had an effect on bending and shear strength.

- Using 12 mm and 25 mm spacing mesh reinforcement instead of steel stirrups in beams under flexural moment (in the steel longitudinal reinforced group) reduced the flexural strength by 17% and 21%, respectively. In the GFRP longitudinal reinforcement group, the use of 12 mm and 25 mm spacing mesh reinforcement instead of steel stirrups increased the flexural strength by 40% and 84%, respectively. It has been evaluated that the interaction of GFRP longitudinal reinforcement and mesh stirrup reinforcement is better.
- In the samples with steel longitudinal reinforcement under shear force, the use of mesh reinforcement instead of steel stirrups increased the shear strength by approximately 13%, but decreased it by 13% and 50% in beams with GFRP.
- It has been observed that increasing the mesh reinforcement spacing is an important advantage for
 workability and placement of concrete, especially in dense fiber concrete types such as SIFCON
 during the concrete casting phase.
- In the samples under shear force, using 12 mm and 25 mm spacing mesh reinforcement instead of stirrup reinforcement increased the energy dissipation capacity by 35% and 53% (in the group with steel longitudinal reinforcement), 16% and 37% (in the group with GFRP longitudinal reinforcement), respectively. On the other hand, the opposite ratio was determined in the samples under the flexural moment. In the steel-reinforced group, the use of mesh reinforcement instead of stirrups decreased the energy dissipation capacity, while it increased the energy dissipation capacity of GFRP beams.

Acknowledgments

I would like to express my sincere gratitude to my esteemed doctoral advisor, Prof. Dr. Abdulkadir Cüneyt AYDIN, for their unwavering support, invaluable guidance, and relentless dedication throughout the course of my research. Their profound insights, expert advice, and constructive feedback have played a pivotal role in shaping the direction of this study.

I would like to extend my heartfelt appreciation to Mahmut Kılıç for his invaluable assistance during the experimental phase. His expertise, dedication, and willingness to lend a helping hand significantly contributed to the successful execution of the experiments.

Conflict of interests

The author(s) declared no potential conflicts of interest with respect to the research, authorship, and/or publication of this article.

Funding

This research received no external funding.

Data availability statement

No new data were created or analyzed in this study.

References

- [1] Akçaözoğlu K, Kıllı A (2021) The effect of curing conditions on the mechanical properties of SIFCON. Revista de la Construcción 20(1):37-51.
- [2] Yoo DY, Kim MJ, Kim S, Ryu GS, Koh KT (2018) Effects of mix proportion and curing condition on shrinkage behavior of HPFRCCs with silica fume and blast furnace slag. Construction and Building Materials 166:241-256.

[3] Uzdil O, Sayın B, Coşgun T (2022) Examination of parameters impacting flexural and shear strengthening of RC beams. J. Struct. Eng. Appl. Mech. 5(3):117-134.

- [4] Ali MH, Atiş CD, Al-Kamaki YSS (2022) Mechanical properties and efficiency of SIFCON samples at elevated temperature cured with standard and accelerated method. Case Studies in Construction Materials 17:01281.
- [5] Balaji S, Thirugnanam G (2018) Behaviour of reinforced concrete beams with SIFCON at various locations in the beam. KSCE Journal of Civil Engineering 22:161-166.
- [6] Arslan ME, Aykanat B, Emiroğlu M (2023) Effects of glass fiber usage on fracture energy and mechanical behavior of concrete: An experimental approach. Journal of Structural Engineering & Applied Mechanics 6(1):70-83.
- [7] Öztekin HF, Gür M, Erdem S, Kaman MO (2022) Effect of fiber type and thickness on mechanical behavior of thermoplastic composite plates reinforced with fabric plies. Journal of Structural Engineering & Applied Mechanics 5(3):161-169.
- [8] Şahan MF, Öncel FA, Ünsal İ (2021) Effect of fiber ratio on the impact behavior of polypropylene fiber reinforced samples. Journal of Structural Engineering & Applied Mechanics 4(4):239-248.
- [9] Lankard DR (1984) Slurry infiltrated fiber concrete (SIFCON): Properties and applications. MRS Online Proceedings Library 42:277-286.
- [10] Al-Abdalay NM, Zeini HA, Kubba HZ (2020) Investigation of the behavior of slurry infiltrated fibrous concrete. Journal of Advanced Research in Fluid Mechanics and Thermal Sciences 65(1):109-120.
- [11] Khamees SS, Kadhum MM, Alwash NA (2021) Effect of hollow ratio and cross-section shape on the behavior of hollow SIFCON columns. Journal of King Saud University-Engineering Sciences 33(3):166-175.
- [12] Mohan A, Karthika S, Ajith J, Tholkapiyan M (2020) Investigation on ultra-high strength slurry infiltrated multiscale fibre reinforced concrete. Materials Today: Proceedings 22:904-911.
- [13] Salih SA, Frayyeh QJ, Ali MAA (2018) Flexural behavior of slurry infiltrated fiber concrete (SIFCON) containing supplementary cementitious materials. Journal of Engineering and Sustainable Development 22(2):35-48.
- [14] Abbas AS, Kadhum MM (2020) Impact of fire on mechanical properties of slurry infiltrated fiber concrete (SIFCON). Civil Engineering Journal 6:12-23.
- [15] Khamees SS, Kadhum MM, Nameer AA (2020) Effects of steel fibers geometry on the mechanical properties of SIFCON concrete. Civil Engineering Journal 6(1):21-33.
- [16] Salih S, Frayyeh Q, Ali M (2018) Fresh and some mechanical properties of SIFCON containing silica fume. In MATEC Web of Conferences EDP Sciences.
- [17] Alhoubi Y, Mahaini Z, Abed F (2022) The flexural performance of BFRP-reinforced UHPC beams compared to steel and GFRP-reinforced beams. Sustainability 14(22):15139.
- [18] Purnell P (2013) The carbon footprint of reinforced concrete. Advances in Cement Research 25(6):362-368.
- [19] Ulger T, Karabulut M, Mert N (2022) Lateral load performance of a reinforced concrete frame with pultruded GFRP box braces. Journal of Structural Engineering & Applied Mechanics (Online) 5(1):40-49.
- [20] Öztürk B, Yılmaz C, Şentürk T (2010) Effect of FRP retrofitting application on seismic behavior of a historical building at Nigde, Turkey. In:14th European Conference on Earthquake Engineering. Ohrid, Republic of Macedonia.
- [21] Kassem MM, Nazri FM, Farsangi EN, Ozturk B (2022) Development of a uniform seismic vulnerability index framework for reinforced concrete building typology. Journal of Building Engineering 47:103838.
- [22] Ozturk B, Senturk T, Yilmaz C (2010) Analytical investigation of effect of retrofit application using CFRP on seismic behavior of a monumental building at historical Cappadocia region of Turkey. In:9th US National and 10th Canadian Conference on Earthquake Engineering. Toronto, Canada.
- [23] Wu C, He X, He L, Zhang J, Wang J (2021) Combination form analysis and experimental study of mechanical properties on steel sheet glass fiber reinforced polymer composite bar. Frontiers of Structural and Civil Engineering 15(4):834-850.
- [24] Wu C, He X, Wu W, Ji K (2023) Low cycle fatigue crack propagation and damage evolution of concrete beams reinforced with GFRP bar. Composite Structures 304:116312.
- [25] Jerry AH, Fawzi NM (2022) The effect of using different fibres on the impact-resistance of slurry infiltrated fibrous concrete (SIFCON). Journal of the Mechanical Behavior of Materials 31(1):135-142
- [26] Sampath P, Asha P (2020) Mechanical properties of slurry infiltrated fibrous concrete (Material) with hooked end fibre. Materials Today: Proceedings 33:2596-2604.

- [27] Sengul O (2018) Mechanical properties of slurry infiltrated fiber concrete produced with waste steel fibers. Construction and Building Materials 186:1082-1091.
- [28] Aygörmez Y, Al-Mashhadani MM, Canpolat O (2020) High-temperature effects on white cement-based slurry infiltrated fiber concrete with metakaolin and fly ash additive. Revista de la Construcción 19(2):324-333.
- [29] Al-Salim NHA, Shwalia ASI, Al-Baghdadi HM (2021) Enhancement energy absorption in flat slabs using slurry infiltrated fibrous concrete. In IOP Conference Series: Materials Science and Engineering. IOP Publishing 1090(1):012026.
- [30] Dong M, Elchalakani M, Karrech A, Pham TM, Yang B (2019) Glass fibre-reinforced polymer circular alkaliactivated fly ash/slag concrete members under combined loading. Engineering Structures 199:109598.
- [31] Ahmed HQ, Jaf DK, Yaseen SA (2020) Comparison of the flexural performance and behaviour of fly-ash-based geopolymer concrete beams reinforced with CFRP and GFRP bars. Advances in Materials Science and Engineering 2020 (10):1-15
- [32] Wang H, Belarbi A (2011) Ductility characteristics of fiber-reinforced-concrete beams reinforced with FRP rebars. Construction and Building Materials 25(5):2391-2401.
- [33] Maranan G, Manalo A, Benmokrane B, Karunasena W, Mendis P (2015) Evaluation of the flexural strength and serviceability of geopolymer concrete beams reinforced with glass-fibre-reinforced polymer (GFRP) bars. Engineering Structures 101:529-541.
- [34] Adam MA, Said M, Mahmoud AA, Shanour AS (2015) Analytical and experimental flexural behavior of concrete beams reinforced with glass fiber reinforced polymers bars. Construction and Building Materials 84:354-366.
- [35] El-Nemr A, Ahmed EA, El-Safty A, Benmokrane B (2018) Evaluation of the flexural strength and serviceability of concrete beams reinforced with different types of GFRP bars. Engineering Structures 17:606-619.
- [36] TS-EN-197-1 (2012) Cement-Part 1: Composition, specification, and conformity criteria for common cements. Turkish Standards Institution, Ankara, Turkiye.
- [37] TS-500-2000 (2000) Turkish Building Code Structural Design, Ankara, Turkiye.
- [38] ACI318-19 (2019) Building code requirements for structural concrete. Farmington Hills, MI, USA: American Concrete Institute.
- [39] TS-EN-12390-3 (2019) Testing hardened concrete Part 3: Compressive strength of test specimens. Ankara, Turkey.
- [40] TS-EN-12390-6 (2010) Testing hardened concrete Part 6: Tensile splitting strength of test specimens. Ankara, Turkey.
- [41] TS-EN-12390-5 (2019) Testing hardened concrete Part 5: Flexural strength of test specimens. Ankara, Turkey.